

Contents lists available at ScienceDirect

Petroleum Science

journal homepage: www.keaipublishing.com/en/journals/petroleum-science



Original Paper

Exploring the mechanisms of calcium carbonate deposition on various substrates with implications for effective anti-scaling material selection



Lu Gong $^{a, b, c, d, 1}$, Fei-Yi Wu $^{d, 1}$, Ming-Fei Pan d , Jun Huang $^{d, e}$, Hao Zhang d , Jing-Li Luo d , Hong-Bo Zeng $^{d, *}$

- ^a College of Science, China University of Petroleum, Beijing, 102249, China
- ^b Beijing Key Laboratory of Optical Detection Technology for Oil and Gas, China University of Petroleum, Beijing, 102249, China
- ^c Basic Research Center for Energy Interdisciplinary, College of Science, China University of Petroleum, Beijing, 102249, China
- d Department of Chemical and Materials Engineering, University of Alberta, Edmonton, Alberta, T6G 1H9, Canada
- ^e Key Laboratory of High Efficiency and Clean Mechanical Manufacture (Ministry of Education), School of Mechanical Engineering, Shandong University, linan. 250061. Shandong. China

ARTICLE INFO

Article history: Received 22 October 2023 Received in revised form 8 January 2024 Accepted 3 February 2024 Available online 5 February 2024

Edited by Min Li

Keywords:
Scaling phenomenon
Metallic substrates
Surface forces
Bulk scaling tests

ABSTRACT

The unexpected scaling phenomena have resulted in significant damages to the oil and gas industries, leading to issues such as heat exchanger failures and pipeline clogging. It is of practical and fundamental importance to understand the scaling mechanisms and develop efficient anti-scaling strategies. However, the underlying surface interaction mechanisms of scalants (e.g., calcite) with various substrates are still not fully understood. In this work, the colloidal probe atomic force microscopy (AFM) technique has been applied to directly quantify the surface forces between calcite particles and different metallic substrates, including carbon steel (CR1018), low alloy steel (4140), stainless steel (SS304) and tungsten carbide, under different water chemistries (i.e., salinity and pH). Measured force profiles revealed that the attractive van der Waals (VDW) interaction contributed to the attachment of the calcium carbonate particles on substrate surfaces, while the repulsive electric double layer (EDL) interactions could inhibit the attachment behaviors. High salinity and acidic pH conditions of aqueous solutions could weaken the EDL repulsion and promote the attachment behavior. The adhesion of calcite particles with CR1018 and 4140 substrates was much stronger than that with SS304 and tungsten carbide substrates. The bulk scaling tests in aqueous solutions from an industrial oil production process showed that much more severe scaling behaviors of calcite was detected on CR1018 and 4140 than those on SS304 and tungsten carbide, which agreed with surface force measurement results. Besides, high salinity and acidic pH can significantly enhance the scaling phenomena. This work provides fundamental insights into the scaling mechanisms of calcite at the nanoscale with practical implications for the selection of suitable antiscaling materials in petroleum industries.

© 2024 The Authors. Publishing services by Elsevier B.V. on behalf of KeAi Communications Co. Ltd. This is an open access article under the CC BY-NC-ND license (http://creativecommons.org/licenses/by-nc-nd/

4.0/).

1. Introduction

The unexpected deposition process of insoluble salt solids from the aqueous solutions onto various facility surfaces, also known as the scaling phenomenon, is a complex and challenging issue in

E-mail address: hongbo.zeng@ualberta.ca (H.-B. Zeng).

numerous industries, such as gas and oil industries (Khormali and Petrakov, 2016; Mpelwa and Tang, 2019; Zhu et al., 2021, 2022). These scaling layers have caused numerous technical problems and

These scaling layers have caused numerous technical problems and accidents. For example, the scaling formation on surfaces of heat exchangers could increase the heat resistance and fluid pressure. The growing scaling layer could also gradually lead to the plugging of pipelines or even the total blockage of the whole conveyance systems (Andritsos and Karabelas, 2003; Sheikholeslami and Watkinson, 1986; Watkinson et al., 1974; Watkinson and Martinez, 1975; Yang et al., 2001). Every year, billions of dollars

^{*} Corresponding author.

¹ L. Gong and F. Wu contribute equally to the work.

have been paid to deal with serious damages and environmental pollution caused by aggravated scaling issues (Müller-Steinhagen et al., 2011; MacAdam and Parsons, 2004). Metallic materials are the most important constructive materials in almost all the industries. They are the basic materials for various production facilities including heat exchangers, liners, tanks, pumps, boilers, wires, and so on (Burakowski and Wierzchon, 1998; Burt, 1995; Froes, 1994; Pandey and Natarajan, 2015). Scaling on metallic surfaces could definitely affect the operations of these facilities and even cause the malfunction of processing facilities in petroleum industries (Abild-Pedersen et al., 2007; Bousselmi et al., 1999; Calle-Vallejo et al., 2012; Hasson et al., 1968; Jain and El-Sayed, 2007). Therefore, it is of practical and fundamental importance to investigate the scaling mechanisms and develop efficient strategies to inhibit scaling processes on various metallic surfaces.

The scalants typically contain the carbonates and sulphates of calcium and magnesium. In certain fields and industries, the barium salts, silicate and phosphate solids could also be discovered in the scaling layers (Chesters, 2009; Kelland, 2011; MacAdam and Parsons, 2004; Shakkthivel and Vasudevan, 2006). Among these components, calcium carbonate or calcite CaCO₃ is one of the major components in the scaling layer (Drever, 1988; Keysar et al., 1994; Tang et al., 2008). Hence, it is reasonable to investigate the scaling mechanisms of calcium carbonate deposited on metallic surfaces as a representative. In literatures, the scale formation could be summarized as a multistep building-up process, including the crystallization of scalant particles in an aqueous solution, the approaching of scalants to the surface from the bulk solution, the adhering of the scalants onto the surface to form the first scale layer, and the growth of the scale sublayers on the surface (Epstein, 1977; Hasson et al., 1997; MacAdam and Parsons, 2004). Obviously, the surface interaction between calcium carbonate and the substrate plays a significantly important role in the approaching and adhering processes to form the first scaling layer, which builds up the foundation for further scaling processes.

In previous research, the primary focus was on mitigating the deposition of calcite on substrate surfaces through chemical and physical methods (Graham et al., 2003; Hasson et al., 2011; Ketrane et al., 2009; MacAdam and Parsons, 2004; Zhou et al., 2020). Chemical scale inhibitors, such as polyphosphates and polyelectrolytes, were incorporated to suppress the formation of calcium carbonate crystals and alleviate scale growth (Amjad, 1988; Butt et al., 1997; Dixon et al., 2020). Besides, various phosphonates have demonstrated great efficiency in impeding the combination of calcium and carbonate ions (Baesso et al., 2023; Mady et al., 2023a, 2023b). Furthermore, magnetic, electronic, and radio frequency devices have been employed to treat aqueous solutions, reducing scalant particles and mitigating calcium carbonate deposition (Cho et al., 1998; Müller-Steinhagen et al., 2011; Santander et al., 2020; Wang et al., 1997). Meanwhile, a mild increase in solution pH has been observed to promote calcium carbonate precipitation, exacerbating scaling phenomena (Andritsos and Karabelas, 1999; Bansal, 1994; Saifelnasr et al., 2013). Recent literatures have explored the adsorption behaviors and mechanisms of chemical inhibitors using advanced nano-mechanical techniques (e.g., atomic force microscopy). These studies reveal that the interactions between inhibitors and calcite surfaces are pivotal to their anti-scaling properties (Dong et al., 2020; Li et al., 2022, 2023; Mohammed et al., 2022). Nevertheless, investigations into the deposition and surface interaction mechanisms of the initial scale layer under diverse conditions, including varying water chemistries, remain significantly limited (Chen et al., 2005; Teng et al., 2017).

In this work, the colloidal probe atomic force microscopy (AFM) technique has been used to directly quantify the surface forces

between calcite particles and various metallic substrates in aqueous solutions with different water chemistries, such as salinity (e.g., 1 and 100 mM NaCl) and solution pH (e.g., 6 and 10). Carbon steels are the most common materials used for the piping and valves in petroleum industries. Low alloy steels are widely applied in the manufacture of various necessary parts such as gears, rams, and spindles. Stainless steels, which are famous for their great resistant ability to corrosion and fouling, are commonly used as construction materials and industrial equipment. The tungsten carbide is one of the representative non-iron-based materials serving as antifouling materials in industries. Hence, four different metallic substrates, including the carbon steel (CR1018), low alloy steel (4140), stainless steel (SS304), and tungsten carbide (carbide), were exploited in the experiments. Furthermore, bulk scaling tests under the same water chemistries were conducted to testify the feasibility of force measurement results. Except for the experiment conditions, an industrial oil processing aqueous solution was included to evaluate the scaling behaviors of calcite particles on different metallic substrates. This work has explored the interaction behaviors of calcium carbonate particles with different metallic surfaces in aqueous solutions to investigate the scaling mechanisms and evaluate their anti-scaling properties, which provides the necessary information for the anti-scaling material section in oil industries.

2. Methodology and experiment

2.1. Materials

The metallic substrates of CR1018, 4140, SS304 and carbide were provided by Reservoir Management Inc. (RGL) with a size of $8 \times 8 \times$ 3 mm. All the substrates were firstly treated with several sand papers to erase the contaminations from the surface and minimize the effect of surface morphologies. Sodium chloride (NaCl, ≥99.5%, Sigma-Aldrich, Canada) was used as the supporting electrolyte. Sodium hydroxide (NaOH, ACS reagent, ≥97%, Sigma-Aldrich, Canada) and hydrochloric acid (HCl, certified ACS Plus, Fisher Scientific, Canada) were used as pH modifiers. Calcium carbonate particles (CaCO₃, Sigma-Aldrich, Canada) were purchased for the AFM probe. Sodium sulphate, sodium bicarbonate, calcium chloride, magnesium chloride, and potassium chloride were all purchased from Sigma-Aldrich and used as received. All the aqueous solutions were prepared using Milli-Q water with a resistivity of 18.2 M Ω cm (BARNSTEAD Smart2Pure, Thermo Scientific, Canada). Ethanol (99.5%, anhydrous, ACROS Organics, Canada) was used as received.

2.2. Surface energies of substrates

The substrates' surface energies have been measured using the Lifshitz-van der Waals Acid/Base approach (Wu et al., 1995). Here, three different liquids were used in the contact angle (CA) measurements, including water (polar liquid), dimethyl sulfoxide (DMSO, partially polar liquid), and diiodomethane (DIM, nonpolar liquid). The surface energies and their parameters of these three probe liquids have been studied and reported in previous literature (Wu et al., 1995). Contact angles in the air were measured with the sessile drop method using a microscope goniometer system (Ramé-Hart instrument, Succasunna, NJ). 5 μL probe liquid was gently dropped on the substrate surface and the images were taken by the software through a camera. Then, the contact angle was read from the recorded image of the software. After the contact angle measurements, the surface energies were calculated using the following equations:

$$\gamma = \gamma^d + \gamma^p = \gamma^d + 2 \cdot \sqrt{\gamma^+ \cdot \gamma^-} \tag{1}$$

where, γ is the total surface energy, γ^d and γ^p are the apolar and polar components, γ^+ is the electron-acceptor parameter, and γ^- is the electron-donor parameter. The surface energy of a substrate can be obtained using Eq. (2).

$$\begin{bmatrix} 2\sqrt{\gamma_{L1}}^{d} & 2\sqrt{\gamma_{L1}}^{+} & 2\sqrt{\gamma_{L1}}^{-} \\ 2\sqrt{\gamma_{L2}}^{d} & 2\sqrt{\gamma_{L2}}^{+} & 2\sqrt{\gamma_{L2}}^{-} \\ 2\sqrt{\gamma_{L3}}^{d} & 2\sqrt{\gamma_{L3}}^{+} & 2\sqrt{\gamma_{L3}}^{-} \end{bmatrix} \cdot \begin{bmatrix} \sqrt{\gamma_{S}}^{d} \\ \sqrt{\gamma_{S}}^{-} \\ \sqrt{\gamma_{S}}^{+} \end{bmatrix} = \begin{bmatrix} \gamma_{L1} \cdot (1 + \cos \theta_{L1}) \\ \gamma_{L2} \cdot (1 + \cos \theta_{L2}) \\ \gamma_{L3} \cdot (1 + \cos \theta_{L3}) \end{bmatrix}$$
(2)

Here, $\gamma_s{}^d$, $\gamma_s{}^+$ and $\gamma_s{}^-$ are the surface energy components of the substrate, $\gamma_L{}^d$, $\gamma_L{}^d$ and $\gamma_L{}^d$ are the surface energy components of the probe liquid, θ_L is the contact angle of probe liquid on the substrate in air.

2.3. Preparation of calcium carbonate probes

The calcium carbonate probes were prepared before the force measurements. The calcium carbonate particles were firstly dispersed in Milli-Q water at the concentration of 1 mg/mL via sonication for 10 min. Then, 100 μL of the dispersion solution was dropped onto a clean glass slide for naturally drying. The two-component epoxy glue (EP2LV, MasterBond, Canada) was prepared and the AFM tipless cantilever (NP–010, Bruker, Santa Barbara, CA) was driven to attach a very small drop of the glue just at the top of the cantilever, followed by picking up a calcium carbonate particle with a size of about 10 μm . The newly custom-made calcium carbonate probes were placed in the air under ambient conditions for at least 24 h before being used in the force measurements. Fig. 1(a) and (b) show the SEM images of a calcium carbonate particle glued on the tipless AFM cantilever.

2.4. AFM force measurements using calcium carbonate probes

The interactions between the calcium carbonate particle and metallic surfaces in aqueous solutions have been directly measured using the AFM colloidal probe technique with a Dimension Icon AFM (Bruker, Santa Barbara, CA), as shown in Fig. 1(c). The spring constant of the probe was obtained using thermal tune method (Cumpson et al., 2004; Hutter and Bechhoefer, 1993). Then, this calcium carbonate probe was used in the following force measurements. Namely, the probe was driven by a piezo actuator to approach a substrate in an aqueous solution at a speed of 1 µm/s till

the maximum loading force of 4 nN was reached. After that, this probe retraced from the surface to the original position. During this process, a laser beam was pointed at the top of the backside of the cantilever. The deflection of this cantilever was monitored by the movement of the reflected laser point at a photo detector. Thus, the force profiles can be calculated from the cantilever deflection and spring constant. The force profile during tracing indicates how calcium carbonate particle approaches and attaches to the substrate surface in an aqueous solution, while the force profile during retracing illustrates the adhering strength of the particle on the surface. For each case, the force measurements are conducted at different spots of one substrate for at least 100 times. One set of force measurements were finished in 30 min to minimize the influence of dissolution and recrystallization processes of calcium carbonate. Before the force measurements, the pre-prepared calcium carbonate probe was firstly applied to measure surface forces with a clean silica substrate in water to ensure the feasibility of calcium carbonate probes. In this work, interaction forces were measured with four metallic substrates in different aqueous solutions.

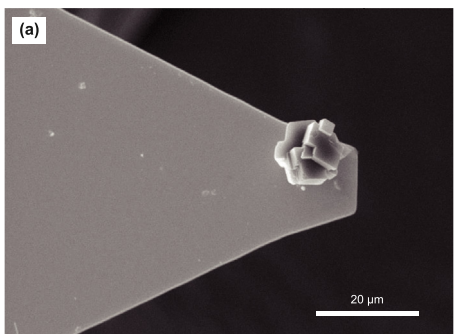
2.5. Bulk scaling tests

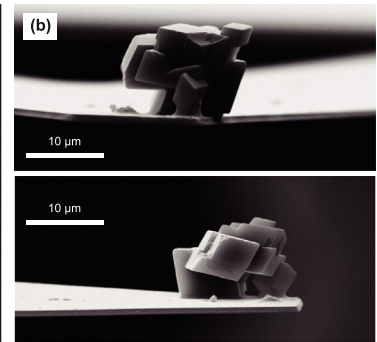
The bulk scaling tests in this work have been conducted to examine the force measurement results. The aqueous solutions were firstly prepared and saturated with CaCO₃ particles (10 mg/mL) for at least 1 day. Then, four metallic substrates were immersed separately in the pre-prepared aqueous solutions with the stirring speed of 300 rpm under ambient condition for 24 h. The substrates were subsequently cleaned with DI water and dried using pure nitrogen. Scanning Electron Microscopy (SEM) and Energy Dispersive X-Ray Spectroscopy (EDS) (VEGA3, TESCAN ANALYTICS, Brno, Czechia) were employed to characterize the scaling phenomena on the metallic substrates. The calcium element from EDS analysis was chosen to evaluate the scaling degree, and the weight percentages of calcium element on all the metallic surfaces were recorded.

3. Results and discussions

3.1. Surface energies of metallic substrates

The contact angles of three probe liquids (water, DMSO and DIM) on CR1018, 4140, SS304 and tungsten carbide substrate in air have been measured and shown in Fig. 2, and the substrates' surface energies are calculated as shown in Table 1. The surface energies of CR1018, 4140, SS304 and carbide are 41.73, 37.67, 34.28 and 50.20 mJ/m², respectively. These values are close to the reported values (Förster et al., 1999; Kalin and Polajnar, 2014;





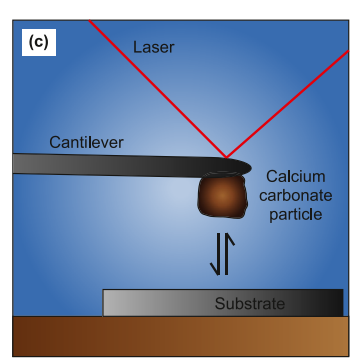


Fig. 1. SEM images of prepared calcium carbonate probe from upper direction (a) and lateral directions (b). (c) Schematic image of the atomic force microscopy (AFM) calcium carbonate probe technique in aqueous solution.

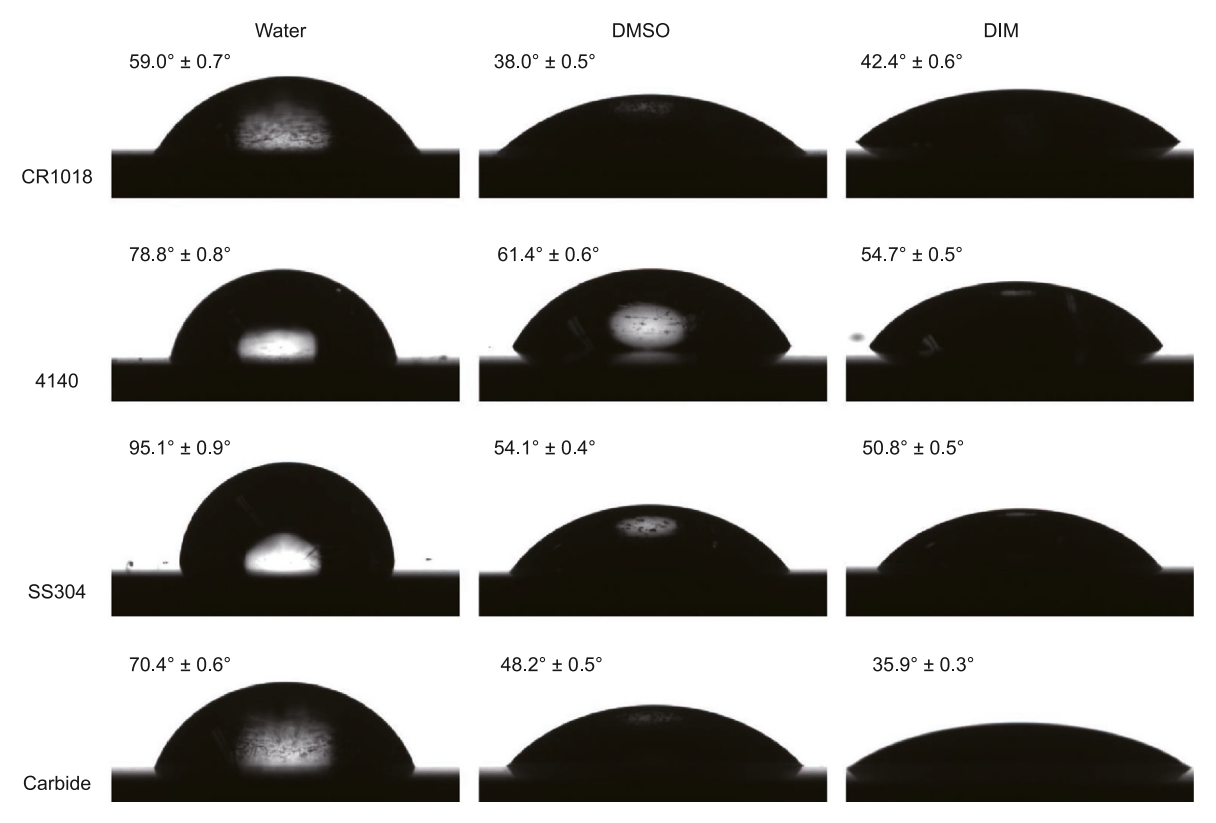


Fig. 2. The contact angles of water, DMSO and DIM on CR1018, 4140, SS304 and tungsten carbide substrate in the air.

Table 1The surface energy of CR1018, 4140, SS304, and tungsten carbide substrate.

Substrate	γ , mJ/m ²	γ^d , mJ/m ²	γ^+ , mJ/m ²	γ^- , mJ/m ²
CR1018	41.73	38.38	0.09	30.24
4140	37.67	31.62	0.53	17.14
SS304	34.28	33.82	0.03	1.84
Tungsten Carbide	50.20	41.61	0.87	21.13

MacAdam and Parsons, 2004; Upadhyaya, 2001). However, it should be noted that measured surface energies are much smaller than theoretically calculated values (Lang and Kohn, 1970; Vitos et al., 1998), which could be due to the inevitable contamination of organics in air and debatable application of three probe liquid technique on metallic surfaces (Forrest et al., 2015; Matsunaga, 1979; Wu et al., 1995). The surface energy of the stainless steel SS304 substrate is the lowest, while the tungsten carbide substrate has the highest surface energy. The CR1018 substrate also has a very high surface energy. Normally, the surface with a greater surface energy should have a stronger binding strength with other materials, such as calcium carbonate (Förster et al., 1999).

3.2. Surface force between calcium carbonate and metallic substrates

The surface interactions between calcium carbonate particles and the metallic substrates (CR1018, 4140, SS304, and tungsten carbide substrate) in aqueous solutions are investigated using the AFM colloidal probe technique. The effects of salinity and pH have been explored here.

Effect of salinity. The salinity in the bulk solution could significantly affect the formation of the electric double layer, which then changes the surface interactions between two substrates

(Israelachvili, 2011). In this part, aqueous solutions with both low (i.e., 1 mM NaCl) and high (i.e., 100 mM NaCl) salinities have been prepared and saturated with calcium carbonate particles before the force measurements. The solution pH was adjusted to the natural pH=6. The measured force profiles with CR1018, 4140, SS304, and tungsten carbide substrates are shown in Fig. 3.

Fig. 3(a) shows the measured interaction force profile between the calcium carbonate and CR1018 substrate in 1 and 100 mM NaCl solution with pH = 6. The orange triangle dots represent the force profile when the calcium carbonate particle was driven to approach the CR1018 substrate in low salinity (i.e., 1 mM NaCl), while the cyan triangle dots are the force profiles during retracing. It is obvious that the tracing force data are positive when the separation becomes less than 10 nm, indicating that the interaction force is repulsive and prevents the calcium carbonate particle from approaching the CR1018 substrate. As the separation distance is less than 4 nm, the force profile suddenly turns to be negative. Namely, a "jump-in" behavior is observed, suggesting that a strong attractive force dominates the interaction force between calcium carbonate and CR1018 within such a small separation range. In the force profile during retracing, the "jump-out" behavior has been detected when the calcium carbonate particle detaches from CR1018 substrate surface, showing a strong adhesion of ~1.0 nN between calcium carbonate and CR1018 substrate. This suggests that the removal of calcium carbonate from CR1018 substrate surface could be difficult. In high salinity (i.e., 100 mM NaCl), the force profile during tracing (i.e., red circles) is almost zero till the separation distance decreases to ~2 nm. A small "jump-in" behavior is also observed due to the attraction between calcium carbonate and CR1018 substrate. This is quite different from the force profiles in low salinity. A strong adhesion of ~0.9 nN has also been detected during retracing (i.e., blue circles). According to the classic Derjaguin-Landau-Vervey-Overbeek (DLVO) theory, the attractive

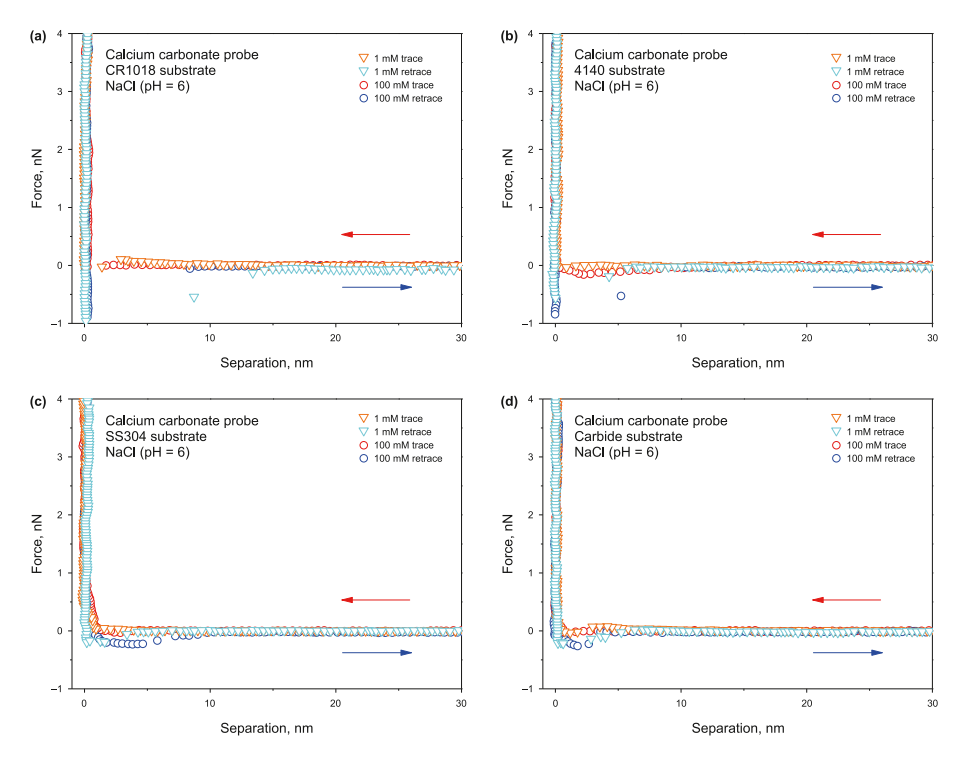


Fig. 3. The measured force profiles of the calcium carbonate probe with **(a)** CR1018, **(b)** 4140, **(c)** SS304 and **(d)** tungsten carbide substrate in 1 and 100 mM NaCl solution with pH = 6.

van der Waals (VDW) force and the repulsive electric double layer (EDL) force are the major contributions to the interaction force between the calcium carbonate and CR1018 substrate in low salinity (i.e., 1 mM NaCl solution) (Israelachvili, 2011). Since the VDW energy decays as a power law with respect to the surface separation distance (i.e. $E_{VDW} \propto 1/D^n$) while the EDL energy decays exponentially (i.e. $E_{\rm EDL} \propto e^{-kD}$), the VDW attraction always overcomes the EDL repulsion when the separation is small enough (Israelachvili, 2011). In low salinity (e.g., 1 mM NaCl), the Debye length is calculated to be 9.6 nm, indicating a strong EDL repulsion between calcium carbonate and substrate surface. This leads to the repulsive force profiles when the calcium carbonate particle approaches CR1018 substrate from a far distance. Then, "jump-in" behavior happens at small separation due to the VDW attraction. However, in high salinity (e.g., 100 mM NaCl), the Debye length is ~0.96 nm. The electric double layer is significantly compressed and the EDL repulsion can be neglected. Therefore, the attractive VDW force is the dominant contribution to the force profiles. Besides, the salinity shows very limited influence on the adhesion strength between calcium carbonate and CR1018 substrate, as the similar adhesion was detected in low and high salinities. When the separation distance decreases to less than 1 nm, the vertical force profiles have been observed in Fig. 3(a), which could be the steric effect due to the rigid surface property of calcium carbonate particles in contact with the CR1018 substrate.

Fig. 3(b)—(d) show the measured force profiles of calcium carbonate particle with 4140, SS304 and tungsten carbide substrate in 1 and 100 mM NaCl solution, respectively. The similar force profiles during tracing have been observed in low salinity, indicating the total contribution of VDW attraction and EDL repulsion. Meanwhile, the force profiles of calcium carbonate with CR1018 substrate and tungsten carbide substrate are more repulsive than those with 4140 substrate and SS304 substrate in low salinity when calcium carbonate particle approaches the substrate, indicating the more difficult attachment process of calcium carbonate particles on

CR1018 substrate and tungsten carbide substrate. Besides, the adhesions have also been detected during retracing, which are ~0.6 nN for 4140 substrate, ~0.3 nN for SS304 substrate, and ~0.3 nN for tungsten carbide substrate, respectively. It is noted that the adhesion with CR1018 substrate is the strongest, and the adhesions with SS304 substrate and tungsten carbide substrate are much weak. Hence, it is easier to remove attached calcium carbonate particles from SS304 substrate and tungsten carbide substrate. In high salinity, all the force profiles during tracing become attractive when calcium carbonate particle approaches the substrate, suggesting the dominant contribution of the VDW force in high salinity. The adhesions during retracing have also been measured to be ~0.8 nN for 4140 substrate, ~0.3 nN for SS304 substrate and ~0.3 nN for tungsten carbide substrate, respectively. Similarly, the CR1018 substrate has the strongest adhesion with calcium carbonate particle, while SS304 substrate and carbide substrate have the weakest adhesion, indicating that the calcium carbonate particle is easy to be removed from tungsten carbide substrate, but difficult from the CR1018 substrate.

Effect of pH. The solution pH is a very important factor in the solubility of calcium carbonate and the surface charge property of a substrate (Shi et al., 2016). In the former part, the interaction forces between calcium carbonate and metallic substrates are measured in NaCl solutions with pH = 6. Here, the effect of basic pH 10 has been investigated. The obtained force profile results are shown in Fig. 4.

Fig. 4(a) shows the measured force profiles between calcium carbonate and CR1018 substrate in 1 and 100 mM NaCl with a basic pH (i.e., pH = 10). The force profile in low salinity exhibits to be repulsive when the separation gets less than ~5 nm. No "jump-in" behavior during tracing has been detected. Compared with the force profiles in low salinity with pH = 6 (Fig. 3(a)), the measured interaction force in basic pH is more repulsive. In high pH, the negatively charged hydroxyl groups can be adsorbed and/or cause deprotonation on the surfaces, which can increase the negative

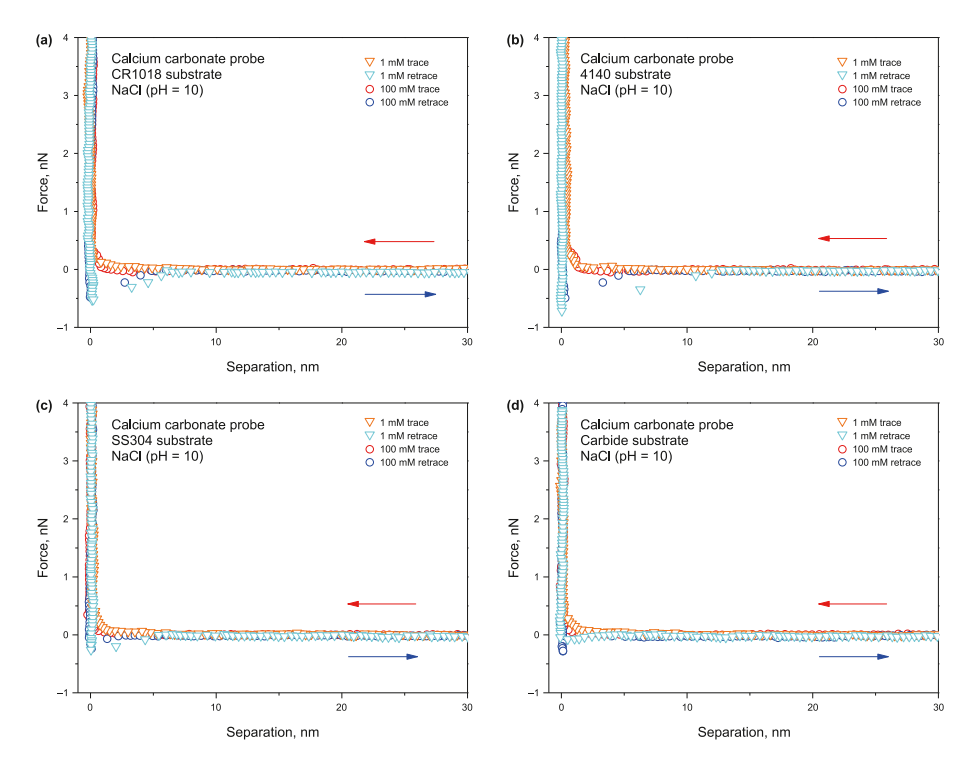


Fig. 4. The measured force profiles of the calcium carbonate probe with (a) CR1018, (b) 4140, (c) SS304 and (d) tungsten carbide substrate in 1 and 100 mM NaCl solution with pH = 10.

charge density on the surface (Israelachvili, 2011; Shi et al., 2016; Xie et al., 2015). Therefore, stronger EDL repulsion between calcium carbonate and CR1018 substrate is observed. During retracing, the adhesion of ~0.5 nN is also detected, which is much weaker than that in pH = 6. This is also attributed to the strengthened EDL repulsion. However, in high salinity (i.e., 100 mM NaCl) with pH = 10, the force profiles during tracing also remain to be zero till the separation distance is less than ~3 nm as the consequence of the highly compressed electric double layer in 100 mM NaCl solution. The adhesion of ~0.5 nN during retracing is also obtained.

Fig. 4(b)-(d) show the measured force profiles of calcium carbonate with 4140, SS304, and tungsten carbide substrate in 1 and 100 mM NaCl with pH = 10. Similarly, the force profiles during tracing show the weak repulsion in low salinity between calcium carbonate and metallic substrate when the separation distance is less than ~5 nm. Meanwhile, the adhesions during retracing are measured to be 0.7 nN for 4140 substrate, 0.3 nN for SS304 substrate, and 0.1 nN for tungsten carbide substrate, respectively. The VDW attraction and EDL repulsion contribute to the measured force results and the EDL repulsion becomes stronger in basic pH (i.e., 10). Hence, compared with the force profiles in Fig. 3(b)–(d), the force profiles during tracing in basic pH are more repulsive and no "jump-in" behavior is observed. The adhesion also becomes a little weaker than that in pH = 6. As to the measured force profiles with 4140, SS304, and tungsten carbide substrates in high salinity with pH 10, since the EDL repulsion is significantly weakened in high salinity, all the force profiles during tracing show no interaction forces between calcium carbonate and metallic substrates till the separation distance is less than ~2 nm. The adhesions are 0.5 nN for 4140 substrate, 0.3 nN for SS304 substrate, and 0.3 nN for tungsten carbide substrate, respectively. It is also noted that the adhesions with CR1018 substrate and 4140 substrate are stronger than those with SS304 substrate and carbide substrate.

Adhesion analysis. The surface forces between calcium carbonate and a metallic substrate (i.e., CR1018, 4140, SS304 or tungsten

carbide substrate) in NaCl solution with different salinity (i.e., 1 and 100 mM) and solution pH (i.e., 6 and 10) have been measured for at least 100 times at different spots of the substrate surfaces in each case. The normalized adhesion forces (adhesion/radius of colloid probe) are listed in Fig. 5.

For a certain substrate (e.g., CR1018 substrate), the measured adhesion becomes a little stronger in high salinity (e.g., 100 mM), but much weaker in basic pH (e.g., pH = 10). High salinity leads to the highly compressed electric double layer, which weakens the

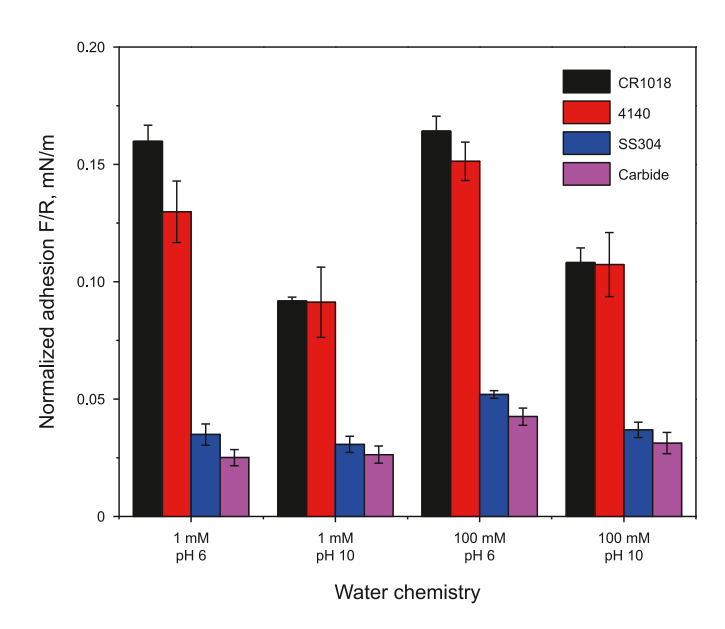


Fig. 5. Measured normalized adhesion of a calcium carbonate with the metallic substrates of CR1018, 4140, SS304 and tungsten carbide substrate in NaCl solutions with different salinity and solution pH.

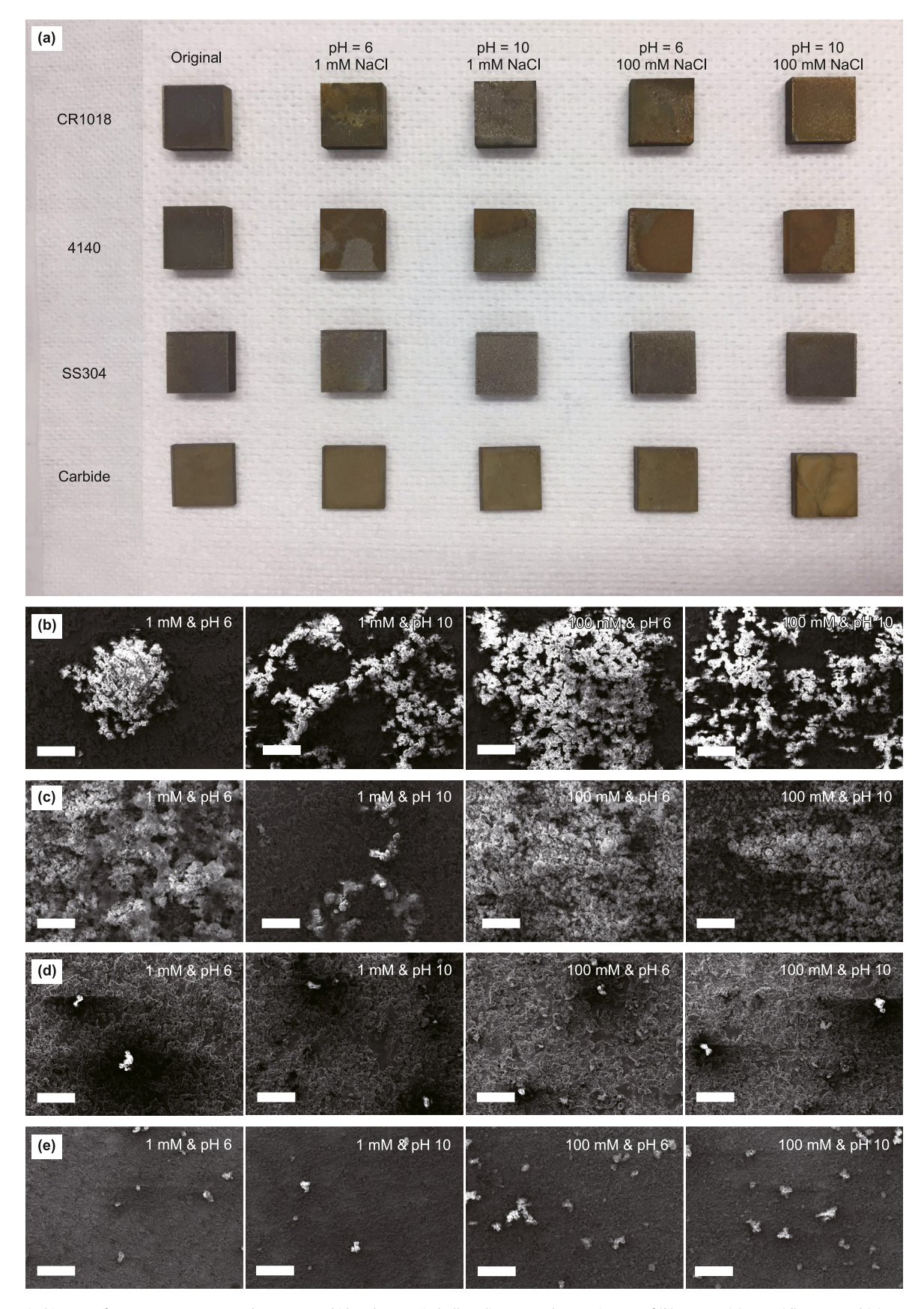


Fig. 6. (a) Optical images of CR1018, 4140, SS304 and tungsten carbide substrates in bulk scaling tests. The SEM images of (b) CR1018, (c) 4140, (d) SS304 and (e) tungsten carbide substrate after bulk scaling tests in NaCl solutions with varying salinity (1 and 100 mM) and solution pH (6 and 10). The white scale bar in each image is 100 μm.

effects of the repulsive EDL force. Basic pH increases the surface potentials of calcium carbonate and metallic substrate in an aqueous solution, resulting in a stronger EDL repulsion. In the same water chemistry (e.g., 1 mM and pH = 6), the adhesions of calcium carbonate with CR1018 and 4140 substrates are much stronger than those with SS304 and tungsten carbide substrates. Compared with SS304 substrate. CR1018 substrate has greater surface free energy. hence owning stronger adhesion with the calcium carbonate (Förster et al., 1999). However, the tungsten carbide substrate has the weakest adhesion, even though the surface energy of the tungsten carbide substrate is quite high. This may be due to the inert chemical activity of carbide materials, which could prevent the formation of stable nuclei on its surface and/or the surface interactions with other materials (Bargir et al., 2009; Kestner and Krueger, 1978; Upadhyaya, 2001; Zhao and Wang, 2005). Conclusively, it is relatively easier for calcium carbonate particles to approach and contact the CR1018 substrate and 4140 substrates, and more difficult to detach from these substrate surfaces. On the contrary, removing calcium carbonate particles from SS304 and tungsten carbide substrates could be much easier.

3.3. Bulk scaling tests

Further bulk scaling tests have been conducted here with CR1018, 4140, SS304, and tungsten carbide substrates in NaCl solutions with varying salinity (i.e., 1 and 100 mM) and solution pH (i.e., 6 and 10). The metallic substrates were immersed in the NaCl solutions with suspended calcium carbonate particles for 24 h. The optical images and SEM images for these metallic substrates are shown in Fig. 6.

In Fig. 6(a), compared with the original substrates, CR1018 and 4140 substrates show some scaling and corrosion on their surfaces after bulk scaling tests. Meanwhile, in high salinity (i.e., 100 mM NaCl), the scaling phenomena are more serious than that in low salinity. On the contrary, no obvious change on SS304 and tungsten carbide substrates has been observed. Fig. 6(b) shows the SEM images of CR1018 substrates after the bulk scaling test in NaCl solution. Obviously, a great number of crystal solids (white area) have been formed on CR1018 substrate surface. Compared with low salinity, more solids have been detected in high salinity (i.e., 100 mM), which could be attributed to the weakened EDL repulsion in high salinity. Meanwhile, the solids aggregate to form large particles on the substrate surface in acidic pH (i.e., 6). In basic pH (i.e., 10), the solids prefer to evenly scatter on the surface. This may be the consequence of strong EDL repulsion between crystals in basic pH. It is also noted that the CR1018 substrate has the most solids after the bulk scaling test in high salinity and acidic pH. The similar scaling phenomena have been found on 4140 substrates as shown in Fig. 6(a) and (c). However, in Fig. 6(a), the SS304 substrates and tungsten carbide substrates still remain clean after bulk scaling tests. The SEM images of these substrates in Fig. 6(d) and (e) also show only several small solids scattering on substrate surfaces. To be more precise, the Energy Dispersive X-Ray Spectroscopy (EDS) is conducted over the area shown in SEM image and the weight percentages of calcium element are chosen to describe the scaling phenomena in Fig. 7. It is noted that a great amount of calcium has been found on CR1018 substrates and 4140 substrates after bulk scaling tests in each case of water chemistry, and much less calcium has been detected on SS304 substrates and tungsten carbide substrates. For a certain substrate, the weight percentage of calcium becomes maximum in high salinity and acidic pH, but minimum in low salinity and basic pH. Conclusively, serious scaling phenomena have occurred on CR1018 substrates and 4140 substrates, while SS304 substrates and tungsten carbide substrates exhibit anti-scaling properties. High salinity and acidic pH can

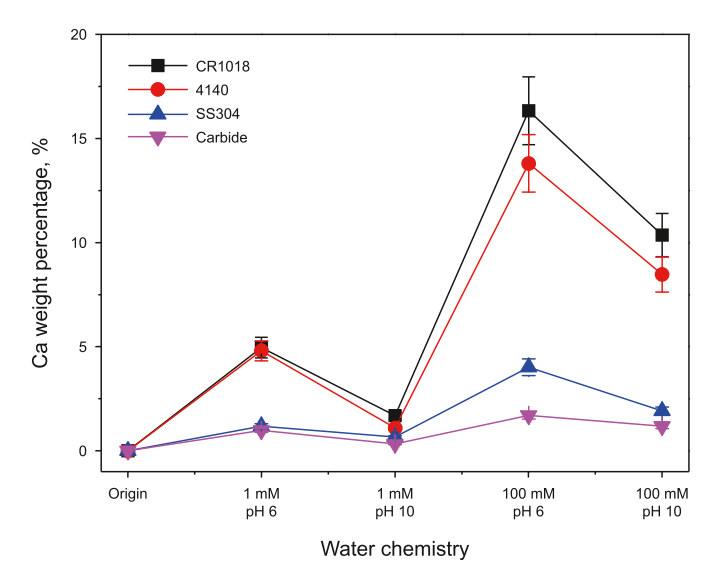


Fig. 7. Weight percentages of calcium element on CR1018, 4140, SS304 and tungsten carbide substrate after bulk scaling tests.

significantly promote scaling processes on metallic substrates. This is consistent with the force measurement results.

3.4. Scaling tests in industrial aqueous solution

To thoroughly investigate the scaling phenomena, it is necessary to conduct scaling tests in an aqueous solution from industrial oil production (denoted as industrial aqueous solution), which is more complex in compositions than lab solutions. The compositions of the industrial aqueous solution during water processing in industries are listed in Table 2 according to the RGL Reservoir Management Inc. The force measurements and bulk scaling tests have been conducted with CR1018, 4140, SS304, and tungsten carbide substrates in the industrial aqueous solution.

Fig. 8(a) shows the obtained force profiles between calcium carbonate and CR1018 substrate in the industrial aqueous solution. The force profile is a weak repulsion when calcium carbonate particle approaches CR1018 substrate within the range of 10 nm due to the EDL repulsion between calcium carbonate and substrate surface. When the separation distance is less than ~2 nm, a "jumpin" behavior is observed, which is attributed to the VDW attraction. During retracing, the strong adhesion of ~0.9 nN is detected. The force profile between calcium carbonate and 4140 substrates in the industrial aqueous solution (Fig. 8(b)) is quite similar to that in Fig. 8(a). Only the "jump-in" behavior during tracing is more significant, indicating that the VDW attraction between calcium carbonate and 4140 substrates is stronger than that with CR1018 substrate. The adhesion of ~0.8 nN is detected during retracing. Fig. 8(c) and (d) show the force profiles of calcium carbonate with SS304 substrate and tungsten carbide substrate. Both force profiles during tracing remain almost zero till the separation is less than 5 nm. The measured adhesions are ~0.4 nN for SS304 substrate and ~0.2 nN for tungsten carbide substrate, respectively. The normalized adhesion between calcium carbonate and metallic substrate after multiple measurements is shown in Fig. 8(e). Obviously,

Table 2 Ion compositions of industrial aqueous solution (pH = 7.4).

Composition	Na ⁺	K^+	Ca ²⁺	Mg^{2+}	Cl-	HCO ₃	SO ₄ ²⁻
Concentration, ppm	434	24	4	1	362	335	161

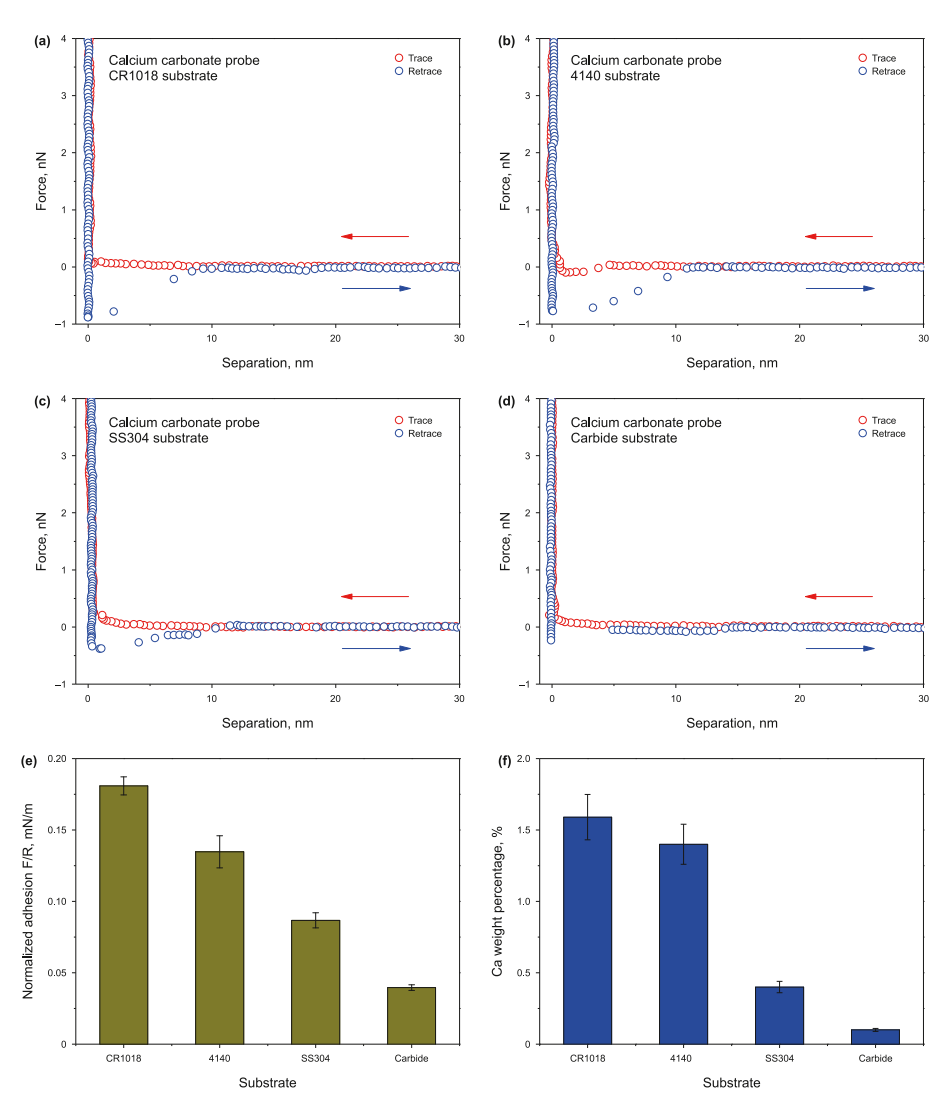


Fig. 8. The typical force curve of calcium carbonate with (a) CR1018, (b) 4140, (c) SS304 and (d) tungsten carbide substrate in industrial aqueous solution, and (e) the measured normalized adhesion for each substrate. (f) The calcium weight percentage on the metallic substrates after bulk scaling tests in the industrial aqueous solution.

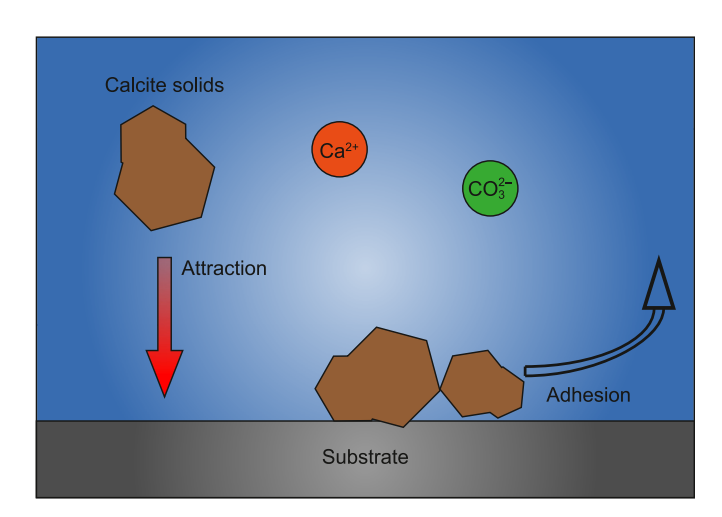


Fig. 9. Schematic illustration of surface interactions in scaling phenomena.

calcium carbonate has the strongest adhesion with CR1018 substrate in the industrial aqueous solution and the weakest adhesion

with the tungsten carbide substrate. Besides, the bulk scaling tests in the industrial aqueous solution are conducted and the metallic substrates are characterized using the SEM and EDS. The calcium weight percentages on these substrates are shown in Fig. 8(f). Clearly, a quite large number of calcium has been detected on CR1018 and 4140 substrates, indicating the serious scaling phenomena on the substrate surface. There is still some calcium carbonate on SS304 substrate after bulk scaling tests. Very limited calcium is present on the tungsten carbide substrate, suggesting the anti-scaling performances of tungsten carbide. These results are in consistence with above conclusions.

4. Conclusions

In this work, the scaling and interaction mechanisms of calcite on metallic substrates have been studied using the AFM force measurements and bulk scaling tests in different aqueous solutions. Four different metallic substrates including carbon steel CR1018, low alloy steel 4140, stainless steel SS304, and tungsten carbide have been investigated here under the effects of salinity and solution pH. Stainless steel SS304 substrate had the lowest surface energy, while tungsten carbide substrate had the highest surface

energy. The force measurement results obtained demonstrated that the attractive van der Waals (VDW) interactions and the repulsive electrical double layer (EDL) repulsion dominated the surface interactions between calcium carbonate particles and metallic substrates. The VDW attraction accelerated the attachment process of calcite particles, leading to exacerbated scaling phenomena (Fig. 9). The repulsive EDL interactions prevented calcium carbonate particles from approaching to substrate surfaces, thus contributing to the anti-scaling property. High salinity could compress the electric double layer and acidic pH led to less negative surface charges, hence weakening the EDL repulsion and promoting the occurrence of the scaling phenomenon. It was also noted that the adhesions of calcium carbonate with CR1018 and 4140 substrates were much stronger than those with SS304 substrate and tungsten carbide substrate. This result indicated that the calcium carbonate particles were more difficult to be detached from CR1018 and 4140 substrates than that from SS304 and tungsten carbide substrates. The bulk scaling tests have demonstrated that, for a selected substrate, aggravated scaling phenomenon of calcium carbonate was detected under high salinity and acidic pH conditions. Meanwhile, more calcium carbonate scaling was observed on CR1018 and 4140 substrates than on SS304 and tungsten carbide substrates. These bulk scaling results were consistent with surface force measurements. This work has improved the useful and fundamental understandings on calcite scaling phenomena and the underlying surface interaction mechanisms under the effects of water chemistries and substrate species, with useful implications for the material selection of efficient anti-scaling performances in various industrial applications. In the future, the scaling behaviors and mechanisms with or without the presence of various scaling inhibitors will be thoroughly investigated using nano-mechanical techniques and molecular dynamic simulations.

CRediT authorship contribution statement

Lu Gong: Writing — review & editing, Writing — original draft, Methodology, Investigation, Formal analysis, Data curation, Conceptualization. **Fei-Yi Wu:** Writing — review & editing, Methodology, Investigation, Data curation. **Ming-Fei Pan:** Writing — review & editing, Methodology, **Jun Huang:** Methodology, Investigation. **Hao Zhang:** Writing — review & editing. **Jing-Li Luo:** Writing — review & editing, Supervision, Project administration, Methodology, Funding acquisition.

Declaration of competing interest

The authors declare that they have no known competing financial interests or personal relationships that could have appeared to influence the work reported in this paper.

Acknowledgement

The authors are grateful to the support from Science Foundation of China University of Petroleum, Beijing (No. 2462023QNXZ018), the Natural Sciences and Engineering Research Council of Canada (NSERC), Canada Foundation for Innovation (CFI), the Research Capacity Program (RCP) of Alberta, and the Canada Research Chairs Program.

References

Abild-Pedersen, F., Greeley, J., Studt, F., et al., 2007. Scaling properties of adsorption energies for hydrogen-containing molecules on transition-metal surfaces. Phys. Rev. Lett. 99 (1), 16105. https://doi.org/10.1103/PhysRevLett.99.016105.

Amjad, Z., 1988. Calcium sulfate dihydrate (gypsum) scale formation on heat exchanger surfaces: the influence of scale inhibitors. J. Colloid Interface Sci. 123 (2), 523–536. https://doi.org/10.1016/0021-9797(88)90274-3.

- Andritsos, N., Karabelas, A., 1999. The influence of particulates on CaCO₃ scale formation. J. Heat Tran. 121 (1), 225–227. https://doi.org/10.1115/1.2825951.
- Andritsos, N., Karabelas, A., 2003. Calcium carbonate scaling in a plate heat exchanger in the presence of particles. Int. J. Heat Mass Tran. 46 (24), 4613–4627. https://doi.org/10.1016/S0017-9310(03)00308-9.
- Baesso, R.C., da Costa, A.C.A., Lutterbach, M.T.S., et al., 2023. Biodegradability assessment of scale inhibitors from oil industry. Petrol. Sci. Technol. 41 (10), 1131–1145. https://doi.org/10.1080/10916466.2022.2075011.
- Bansal, B., 1994. Crystallisation Fouling in Plate Heat Exchangers. ResearchSpace@ Auckland.
- Bargir, S., Dunn, S., Jefferson, B., et al., 2009. The use of contact angle measurements to estimate the adhesion propensity of calcium carbonate to solid substrates in water. Appl. Surf. Sci. 255 (9), 4873–4879. https://doi.org/10.1016/ i.apsusc.2008.12.017.
- Bousselmi, L., Fiaud, C., Tribollet, B., et al., 1999. Impedance spectroscopic study of a steel electrode in condition of scaling and corrosion: interphase model. Electrochim. Acta 44 (24), 4357–4363. https://doi.org/10.1016/S0013-4686(99)
- Burakowski, T., Wierzchon, T., 1998. Surface Engineering of Metals: Principles, Equipment, Technologies. CRC press.
- Burt, R., 1995. The transformation of the non-ferrous metals industries in the seventeenth and eighteenth centuries. Econ. Hist. Rev. 23–45. https://doi.org/10.2307/2597869
- Butt, F., Rahman, F., Baduruthamal, U., 1997. Evaluation of SHMP and advanced scale inhibitors for control of CaSO₄, SrSO₄, and CaCO₃ scales in RO desalination. Desalination 109 (3), 323–332. https://doi.org/10.1016/S0011-9164(97)00078-7
- Calle-Vallejo, F., Martínez, J., García-Lastra, J.M., et al., 2012. Physical and chemical nature of the scaling relations between adsorption energies of atoms on metal surfaces. Phys. Rev. Lett. 108 (11), 116103. https://doi.org/10.1103/ PhysRevLett.108.116103.
- Chen, S., Zheng, J., Li, L., et al., 2005. Strong resistance of phosphorylcholine self-assembled monolayers to protein adsorption: insights into nonfouling properties of zwitterionic materials. J. Am. Chem. Soc. 127 (41), 14473—14478. https://doi.org/10.1021/ja054169u.
- Chesters, S.P., 2009. Innovations in the inhibition and cleaning of reverse osmosis membrane scaling and fouling. Desalination 238 (1–3), 22–29. https://doi.org/10.1016/j.desal.2008.01.031.
- Cho, Y., Fan, C., Choi, B.-G., 1998. Use of electronic anti-fouling technology with filtration to prevent fouling in a heat exchanger. Int. J. Heat Mass Tran. 41 (19), 2961–2966. https://doi.org/10.1016/S0017-9310(98)00011-8.
- Cumpson, P.J., Zhdan, P., Hedley, J., 2004. Calibration of AFM cantilever stiffness: a microfabricated array of reflective springs. Ultramicroscopy 100 (3–4), 241–251. https://doi.org/10.1016/j.ultramic.2003.10.005.
- Dixon, D.V., Stoyanov, S.R., Xu, Y., et al., 2020. Challenges in developing polymer flocculants to improve bitumen quality in non-aqueous extraction processes: an experimental study. Petrol. Sci. 17, 811–821. https://doi.org/10.1007/s12182-019-00414-z.
- Dong, S., Berelson, W.M., Adkins, J.F., et al., 2020. An atomic force microscopy study of calcite dissolution in seawater. Geochem. Cosmochim. Acta 283, 40–53. https://doi.org/10.1016/j.gca.2020.05.031.
- Drever, J.I., 1988. The Geochemistry of Natural Waters, 437. prentice Hall, Englewood Cliffs.
- Epstein, N., 1977. Fouling in Heat Exchangers, Sixth International Heat Transfer Conference, pp. 235–253.
- Forrest, E., Schulze, R., Liu, C., et al., 2015. Influence of surface contamination on the wettability of heat transfer surfaces. Int. J. Heat Mass Tran. 91, 311–317. https://doi.org/10.1016/j.ijheatmasstransfer.2015.07.112.
- Förster, M., Augustin, W., Bohnet, M., 1999. Influence of the adhesion force crystal/heat exchanger surface on fouling mitigation. Chem. Eng. Process: Process Intensif. 38 (4–6), 449–461. https://doi.org/10.1016/S0255-2701(99)00042-2.
- Froes, F., 1994. Advanced metals for aerospace and automotive use. Mater. Sci. Eng., A 184 (2), 119–133. https://doi.org/10.1016/0921-5093(94)91026-X.
- Graham, G., Boak, L., Sorbie, K., 2003. The influence of formation calcium and magnesium on the effectiveness of generically different barium sulphate oil-field scale inhibitors. SPE Prod. Facil. 18 (1), 28–44. https://doi.org/10.2118/81825-PA.
- Hasson, D., Avriel, M., Resnick, W., et al., 1968. Mechanism of calcium carbonate scale deposition on heat-transfer surfaces. Ind. Eng. Chem. Fundam. 7 (1), 59–65. https://doi.org/10.1021/i160025a011.
- Hasson, D., Bramson, D., Limoni-Relis, B., et al., 1997. Influence of the flow system on the inhibitory action of CaCO₃ scale prevention additives. Desalination 108 (1–3), 67–79. https://doi.org/10.1016/S0011-9164(97)00010-6.
- Hasson, D., Shemer, H., Sher, A., 2011. State of the art of friendly "green" scale control inhibitors: a review article. Ind. Eng. Chem. Res. 50 (12), 7601–7607. https://doi.org/10.1021/ie200370v.
- Hutter, J.L., Bechhoefer, J., 1993. Calibration of atomic-force microscope tips. Rev. Sci. Instrum. 64 (7), 1868–1873. https://doi.org/10.1063/1.1143970.
- Israelachvili, J.N., 2011. Intermolecular and Surface Forces. Academic press.
- Jain, P.K., El-Sayed, M.A., 2007. Surface plasmon resonance sensitivity of metal nanostructures: physical basis and universal scaling in metal nanoshells. J. Phys. Chem. C 111 (47), 17451–17454. https://doi.org/10.1021/jp0773177.

Kalin, M., Polajnar, M., 2014. The wetting of steel, DLC coatings, ceramics and polymers with oils and water: the importance and correlations of surface energy, surface tension, contact angle and spreading. Appl. Surf. Sci. 293, 97–108. https://doi.org/10.1016/j.apsusc.2013.12.109.

- Kelland, M.A., 2011. Effect of various cations on the formation of calcium carbonate and barium sulfate scale with and without scale inhibitors. Ind. Eng. Chem. Res. 50 (9), 5852–5861. https://doi.org/10.1021/ie2003494.
- Kestner, M.O., Krueger, R.H., 1978. Scale resistant heat transfer surfaces and a method for their preparation. Google Patents.
- Ketrane, R., Saidani, B., Gil, O., et al., 2009. Efficiency of five scale inhibitors on calcium carbonate precipitation from hard water: effect of temperature and concentration. Desalination 249 (3), 1397–1404. https://doi.org/10.1016/ i.desal.2009.06.013.
- Keysar, S., Semiat, R., Hasson, D., et al., 1994. Effect of surface roughness on the morphology of calcite crystallizing on mild steel. J. Colloid Interface Sci. 162 (2), 311–319. https://doi.org/10.1006/jcis.1994.1044.
- Khormali, A., Petrakov, D.G., 2016. Laboratory investigation of a new scale inhibitor for preventing calcium carbonate precipitation in oil reservoirs and production equipment. Pet. Sci. 13, 320–327. https://doi.org/10.1007/s12182-016-0085-6.
- Lang, N., Kohn, W., 1970. Theory of metal surfaces: charge density and surface energy. Phys. Rev. B 1 (12), 4555. https://doi.org/10.1103/PhysRevB.1.4555.
- Li, A., Chang, J., Shui, T., et al., 2023. Probing interaction forces associated with calcite scaling in aqueous solutions by atomic force microscopy. J. Colloid Interface Sci. 633, 764–774. https://doi.org/10.1016/j.jcis.2022.11.114.
- Li, A., Zhang, H., Liu, Q., et al., 2022. Effects of chemical inhibitors on the scaling behaviors of calcite and the associated surface interaction mechanisms. J. Colloid Interface Sci. 618, 507–517. https://doi.org/10.1016/j.jcis.2022.03.105.
- MacAdam, J., Parsons, S.A., 2004. Calcium carbonate scale formation and control. Rev. Environ. Sci. Biotechnol. 3 (2), 159–169. https://doi.org/10.1007/s11157-004-3849-1.
- Mady, M.F., Abdelaal, A.T., Kelland, M.A., et al., 2023a. Flexible, linear, and systematically expanded tetraphosphonate bolaamphiphiles and their inhibition performance against calcite and barite scale formation. Energy Fuels 37 (13), 9176–9184. https://doi.org/10.1021/acs.energyfuels.3c01428.
- Mady, M.F., Abdelaal, A.T., Moschona, A., et al., 2023b. Systematic molecular-size variants in diphosphonate inhibitors for oilfield scale management. Energy Fuels 37 (6), 4365–4376. https://doi.org/10.1021/acs.energyfuels.2c04277.
- Matsunaga, T., 1979. Relationship between Surface Energy and Surface Contamination, Surface Contamination. Springer, pp. 47–56.
- Mohammed, I., Isah, A., Al Shehri, D., et al., 2022. Effect of sulfate-based scales on calcite mineral surface chemistry: insights from zeta-potential experiments and their implications on wettability. ACS Omega 7 (32), 28571–28587. https://doi.org/10.1021/acsomega.2c03403.
- Mpelwa, M., Tang, S.-F., 2019. State of the art of synthetic threshold scale inhibitors for mineral scaling in the petroleum industry: a review. Pet. Sci. 16, 830–849. https://doi.org/10.1007/s12182-019-0299-5.
- Müller-Steinhagen, H., Malayeri, M.R., Watkinson, A.P., 2011. Heat exchanger fouling: mitigation and cleaning strategies. Heat Tran. Eng. 32 (3–4), 189–196. https://doi.org/10.1080/01457632.2010.503108.
- Pandey, B., Natarajan, K., 2015. Microbiology for Minerals, Metals, Materials and the Environment. CRC Press.
- Saifelnasr, A., Bakheit, M., Kamal, K., et al., 2013. Calcium carbonate scale formation, prediction and treatment (case study gumry oilfield-pdoc). Int. Lett. Chem. Phys. Astron. 12. https://doi.org/10.18052/www.scipress.com/ILCPA.17.47.

- Santander, C., Liu, J., Tan, X., et al., 2020. Destabilization of bitumen-coated fine solids in oil through water-assisted flocculation using biomolecules extracted from guar beans. Pet. Sci. 17, 1726–1736. https://doi.org/10.1007/s12182-020-00491-5.
- Shakkthivel, P., Vasudevan, T., 2006. Acrylic acid-diphenylamine sulphonic acid copolymer threshold inhibitor for sulphate and carbonate scales in cooling water systems. Desalination 197 (1–3), 179–189. https://doi.org/10.1016/j.desal.2005.12.023.
- Sheikholeslami, R., Watkinson, A., 1986. Scaling of plain and externally finned heat exchanger tubes. J. Heat Tran. 108 (1), 147–152. https://doi.org/10.1115/1.3246879.
- Shi, C., Zhang, L., Xie, L., et al., 2016. Interaction mechanism of oil-in-water emulsions with asphaltenes determined using droplet probe AFM. Langmuir 32 (10), 2302–2310. https://doi.org/10.1021/acs.langmuir.5b04392.
- Tang, Y., Yang, W., Yin, X., et al., 2008. Investigation of CaCO₃ scale inhibition by PAA, ATMP and PAPEMP. Desalination 228 (1–3), 55–60. https://doi.org/10.1016/i.desal.2007.08.006.
- Teng, K.H., Kazi, S.N., Amiri, A., et al., 2017. Calcium carbonate fouling on doublepipe heat exchanger with different heat exchanging surfaces. Powder Technol. 315, 216–226. https://doi.org/10.1016/j.powtec.2017.03.057.
- Upadhyaya, G.S., 2001. Materials science of cemented carbides—an overview. Mater. Des. 22 (6), 483–489. https://doi.org/10.1016/S0261-3069(01)00007-3.
- Vitos, L., Ruban, A., Skriver, H.L., et al., 1998. The surface energy of metals. Surf. Sci. 411 (1–2), 186–202. https://doi.org/10.1016/S0039-6028(98)00363-X.
- Wang, Y., Babchin, J., Chernyi, L., et al., 1997. Rapid onset of calcium carbonate crystallization under the influence of a magnetic field. Water Res. 31 (2), 346–350. https://doi.org/10.1016/S0043-1354(96)00243-6.
- Watkinson, A., Louis, L., Brent, R., 1974. Scaling of enhanced heat exchanger tubes. Can. J. Chem. Eng. 52 (5), 558–562. https://doi.org/10.1002/cjce.5450520503.
- Watkinson, A., Martinez, O., 1975. Scaling of heat exchanger tubes by calcium carbonate. J. Heat Tran. 97 (4), 504–508. https://doi.org/10.1115/1.3450419.
- Wu, W., Giese, R.J., Van Oss, C., 1995. Evaluation of the Lifshitz-van der Waals/acid-base approach to determine surface tension components. Langmuir 11 (1), 379–382. https://doi.org/10.1021/la00001a064.
- Xie, L., Shi, C., Wang, J., et al., 2015. Probing the interaction between air bubble and sphalerite mineral surface using atomic force microscope. Langmuir 31 (8), 2438–2446. https://doi.org/10.1021/la5048084.
- Yang, Q., Liu, Y., Gu, A., et al., 2001. Investigation of calcium carbonate scaling inhibition and scale morphology by AFM. J. Colloid Interface Sci. 240 (2), 608–621. https://doi.org/10.1006/jcis.2001.7669.
- Zhao, Q., Wang, X., 2005. Heat transfer surfaces coated with fluorinated diamond-like carbon films to minimize scale formation. Surf. Coating. Technol. 192 (1), 77–80. https://doi.org/10.1016/j.surfcoat.2004.02.030.
- Zhou, M., Gu, Y., Yi, R., et al., 2020. Synthesis and property study of ter-copolymer P (MA-AMPS-HPA) scale inhibitor. J. Polym. Res. 27, 1–12. https://doi.org/10.1007/s10965-020-02270-7
- Zhu, M.L., Qian, H.J., Fan, W.H., et al., 2022. Surface lurking and interfacial ion release strategy for fabricating a superhydrophobic coating with scaling inhibition. Pet. Sci. 19 (6), 3068–3079. https://doi.org/10.1016/j.petsci.2022.07.005.
- Zhu, M.L., Qian, H.J., Yuan, R.X., et al., 2021. EDTA interfacial chelation Ca²⁺ incorporates superhydrophobic coating for scaling inhibition of CaCO₃ in petroleum industry. Pet. Sci. 18, 951–961. https://doi.org/10.1007/s12182-021-00558-x.